Fu, J.; Quast, T.; Velke, E.; Esslinger, M.; Pastuschek, M.; Schirmacher, A.; Aschan, R.; Manoocheri, F.; Ikonen, E.

Development of primary reference facilities and measurement comparison of standard artifacts for the bidirectional transmittance distribution function

Published in:
Review of Scientific Instruments

DOI:
10.1063/5.0151803

Published: 01/08/2023

Document Version
Publisher's PDF, also known as Version of record

Metrologia

PAPER • OPEN ACCESS

Phase-stepping interferometry for parallelism measurement of step gauge faces

To cite this article: Sucheta Sharma *et al* 2023 *Metrologia* **60** 055004

OPEN ACCESS
IOP Publishing | Bureau International des Poids et Mesures Metrologia
Metrologia **60** (2023) 055004 (12pp) https://doi.org/10.1088/1681-7575/ace7d5

Phase-stepping interferometry for parallelism measurement of step gauge faces

Sucheta Sharma[1,*], **Johan Nysten**[2], **Antti Lassila**[2] **and Erkki Ikonen**[1,2]

[1] Metrology Research Institute, Aalto University, Maarintie 8, 02150 Espoo, Finland
[2] VTT MIKES, VTT Technical Research Centre of Finland Ltd, Tekniikantie 1, 02150 Espoo, Finland

E-mail: sucheta.sharma@aalto.fi

Received 24 May 2023, revised 21 June 2023
Accepted for publication 17 July 2023
Published 4 August 2023

Abstract
The article presents a measurement method driven with a non-contact optical system consisting of a mirror array by employing phase stepping interferometry to determine the surface parallelism of step gauge faces. The array houses a prism mirror to allow simultaneous interferometric measurement of two opposite step gauge faces relative to the front surface. Mechanical movement of the mirror array is detected using an alignment monitoring mirror to compensate the tilt angle of the system. The front surface of the step gauge and the alignment mirror, located at the measurement arm of the interferometer, are adjusted normal to the collimated laser beam of 50 mm diameter. Phase stepping is performed by a piezo controlled mirror at the reference arm. A theoretical approach is described to verify the experimentally obtained sensitivities of the system due to yaw and pitch misalignments of the mirror array and the step gauge. The technique offers improved measurement accuracy to measure the parallelism of the step gauge faces. Main uncertainty components are caused by the plane fitting analysis of non-ideal surfaces and repeatability of the results. The combined standard uncertainty of parallelism measurement is 18 μrad.

Keywords: step gauge, interferometer, non-contact measurement, phase-stepping, alignment sensitivity

(Some figures may appear in colour only in the online journal)

1. Introduction

Step gauges are versatile transfer standards of length, needed for various purposes. A step gauge is constituted by gauge blocks for which established non-contact measurement methods for length and surface parallelism are available [1–3]. However, because of the structure of a step gauge, such measurement approach is not very common for step gauges, and development is still needed in this field. Step gauges are important for calibrating instruments including calipers, height gauges and co-ordinate measuring machines (CMMs) [4, 5]. In order to perform measurements that are traceable to the SI-meter, the employed step gauge should be calibrated [6]. Tactile measurement techniques are generally well-known for carrying out associated precision measurements and calibration tasks [7–9].

The most important measurand of a step gauge is the face spacing, i.e., the distance of each step gauge face from the reference face. Measurements, in such context, are usually carried out along a defined axis. The measurement axis can be set correctly, for example in CMMs, using the frame geometry of

* Author to whom any correspondence should be addressed.

the step gauge and other parameters given by the manufacturer. In addition to the face spacing, the parallelism of the surfaces is important for the step gauge. Parallelism error has direct influence on the accuracy with which one can use the step gauge for transferring the SI-meter to another instrument [4]. CMMs operate with spherical probes with which it is possible to set the measurement line within a few µm of the correct position. Under this condition, the parallelism error has negligible effect. However, e.g., when calibrating height gauges with flat anvils, the probing point is the highest point in line of contact and the amount of error in parallelism directly affects the reading of the gauge. CMMs generally work with an auxiliary laser interferometer to calibrate step gauges. For such setups, the parallelism of the face is mainly measured by probing several points on each surface. Most accurate calibrations for step gauges are performed with custom-made interferometers with a probing unit [10–13]. These setups provide improved accuracy, however, parallelism measurement requires readjustments of the step gauge with offset re-estimation and repetition of the measurements.

Kruger [14, 15] proposed a method employing phase-shifting flatness interferometer and a periscope system to measure the step gauge flatness and parallelism. The accuracy for such system relies on the guided movement of the periscope along the measurement axes. Hence, determining the measurement error introduced due to misalignments is important to improve the accuracy.

In this work, we present an improved optical arrangement for parallelism measurement. The new design of the custom-tailored optical system with a mirror array and an additional alignment monitoring mirror is the key to identify and compensate errors due to misalignment of the system. We studied the suitability of this method to measure the parallelism of step gauge faces. We carried out a thorough experimental and theoretical analysis on the alignment sensitivities of the optical system which influences the measurement accuracy of the setup. To our knowledge, correction of the effect of the misalignment of the mirror array in parallelism measurement using our method has not been reported before. The following sections contain the theoretical and experimental descriptions of sensitivity estimation and parallelism measurement process.

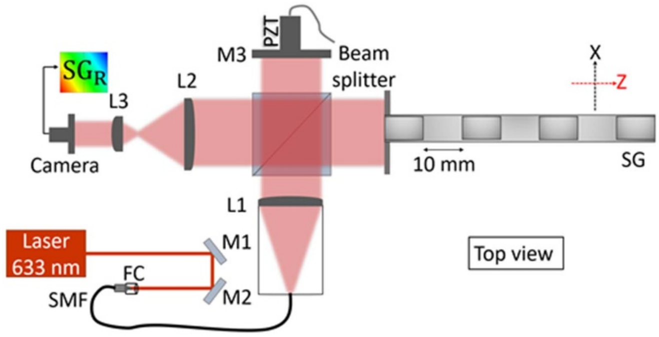

Figure 1. Experimental setup (top view) for the measurements of step gauge (SG) parallelism: Michelson type interferometer with phase stepping process actuated by a piezo (PZT) driven mirror (M3) stage. The measurement arm of the interferometer contains the SG. The unwrapped phase image of the SG reference front surface (SG_R) is shown as the camera output.

2. Experimental methods and measurement procedure

Figure 1 shows the experimental setup which is based on a Michelson interferometer with a Zeeman stabilized 633 nm He–Ne laser source. The free-space laser input is first coupled into a single mode fiber (SMF) by a fiber-optic coupler (FC). The output of the SMF is connected to a collimation and beam size expansion section which comprises of a length extendable tube and a plano-convex lens of 50 mm diameter. The length of the extendable lens tube is adjusted with a shearing interferometer to achieve good collimation. The collimated beam is directed to a 50 mm cubic beam splitter which produces transmitted beam to the reference arm and reflected beam to the measurement arm of the interferometer. The outer surfaces of the beam splitter are slightly deviated from normal incidence of the light beam. In addition, the beam splitter surfaces have anti-reflection coatings, hence, the disturbances due to additional reflections are reduced. The reference arm is ended by a piezo driven mirror and the step gauge is positioned in the measurement arm. Figure 1 shows the measurement condition when only the step gauge front surface receives the target beam. In order to measure other step gauge faces, an array of mirrors arranged as a periscope and a triangular prism reflector-type configuration is used.

Figure 2 illustrates the optical system consisting of the alignment mirror (M5) and the mirror array with the setup where the measurement beam is reflected by mirror M5 and the above-mentioned array of mirrors: M4, M6 and M7. The back-reflected measurement beam contains phase information of four surfaces as shown in figure 2: (a) M7 and M6 provide the surface information of the even and odd faces of the step gauge, i.e., SG_{Ei} and SG_{Oi} (where i is the face number of the step gauge, i.e., $i = 2, 3, 4\ldots$), which are positioned after the step gauge reference surface, SG_R; (b) M5 monitors the angular alignment of the mirror array; (c) beam reflected by SG_R shows the first step gauge face (i.e., $i = 1$) with respect to which the parallelism of the other surfaces is measured.

Finally, the interferograms are recorded by a monochrome camera after adapting the beam size by a telescope with two plano-convex lenses of diameters 50 mm and 12 mm (as shown in figure 1). The camera and the piezo stage are connected to the measurement computer to monitor and control the phase stepping process.

2.1. Alignment process of the optical system

Before carrying out the surface parallelism tests, the optical system was aligned properly, and the residual errors were characterized (figure 3). First, the reference arm mirror M3 was aligned normal to the incident beam when having a precision corner cube (CC) with beam deviation specification of <10 µrad at the measurement arm. After aligning the piezo driven reference mirror M3, the CC was removed, and a flat

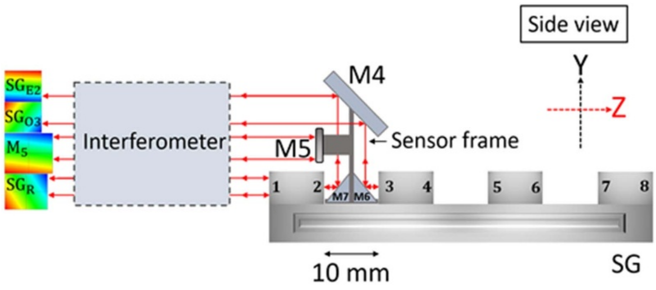

Figure 2. Schematic representation of the optical system (side view). Mirror M4 directs the beam to the reflectors M7 and M6 which provide information about the step gauge (SG) even and odd surfaces facing them. Mirror M5 is the alignment monitoring mirror which is an important component to identify any yaw and pitch misalignment of the optical system during mechanical movements. The diagram represents how the first (SG_R), second (SG_{E2}) and third (SG_{O3}) faces of the SG, along with the alignment mirror (M_5) of the optical system, can be simultaneously monitored by observing the unwrapped phase images.

mirror representing SG_{O3} was placed at the measurement arm. This flat mirror was aligned normal to the beam and residual angular deviation was measured with the phase stepping method (figure 3(a)). Next, another flat mirror representing step gauge surface SG_{E2} was placed to reflect in the opposite direction as compared with the first mirror. Then the precision CC was mounted to face the latter mirror which was adjusted to normal incidence and residual angular error was measured with the phase stepping method (figure 3(b)). After that, the CC was removed, and the optical system with the mirror array and the alignment mirror was positioned between those two auxiliary mirrors for adjustment (figure 3(c)). In this position, mirror M5 and the mirror array: M4, M6, M7, were adjusted as well as possible to provide reflections corresponding to normal beam incidence at the auxiliary mirrors. After that, residual angular offsets of M5 and the mirrors analogous to SG_{E2} and SG_{O3} were measured with phase stepping. The obtained residual offset angles are employed to compensate for the remaining alignment errors in the actual measurements.

2.2. Phase stepping method for surface tilt measurement

The phase stepping method [16, 17], where the change in optical path length between the interfering beams is introduced with equal steps, was used for surface tilt measurements. Before starting the measurement, the piezo stage was calibrated to identify the control voltages that make $\pi/2$ phase steps. During data collection, an automated measurement program shifts the phase by $\pi/2$ and produces at each phase a dataset with the recorded interferograms. The SG_R, SG_{Ei}, SG_{Oi} and M_5 areas are analyzed separately. The 9-point algorithm is employed to provide one wrapped phase image. Then the phase images of the surface areas are unwrapped to retrieve the surface topography information [16, 17]. A central region on each surface is considered for further data analysis. A plane fit is applied on the phase unwrapped data of the region (figure 4) from which the surface tilt is determined.

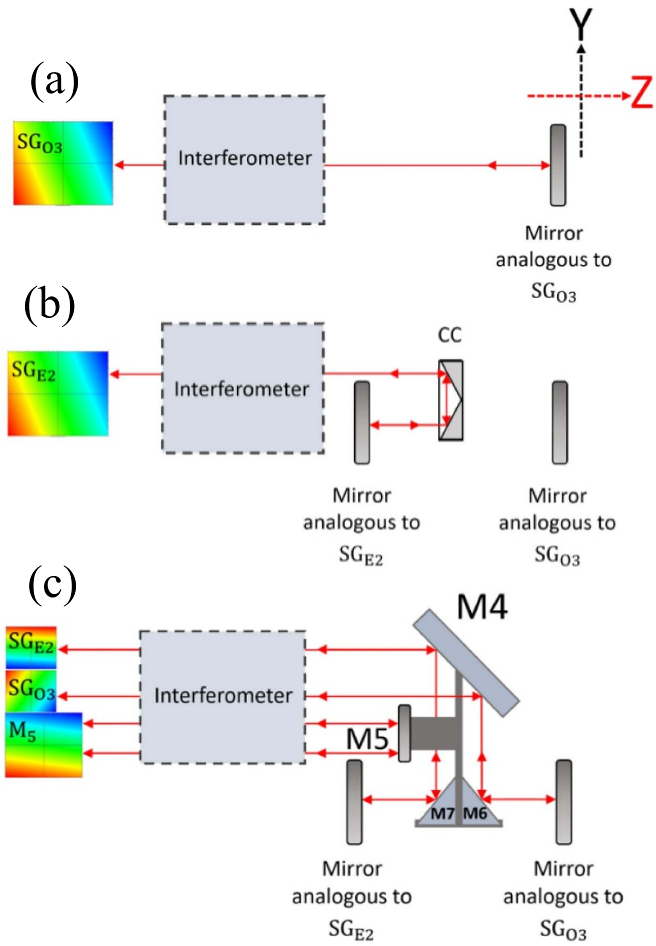

Figure 3. (a)–(c) Schematic diagram of the experimental setups for adjusting the optical system with the alignment mirror and the mirror array to determine the offset.

The values of yaw (ψ) and pitch (θ) tilt of each surface are measured from the plane fitted data by calculating the slope i.e., the total interferometric phase change over the total length of the pixel range. The blue and red lines of the horizontal and vertical profile graphs of the corresponding phase maps, as shown in figure 4(b), indicate the interference phase changes $\Delta\varphi_H$ and $\Delta\varphi_V$ in rad, due to yaw and pitch, respectively. Equations (1) and (2) are employed to calculate ψ and θ,

$$\psi = \frac{\Delta\varphi_H \lambda}{4\pi L_H} \tag{1}$$

$$\theta = \frac{\Delta\varphi_V \lambda}{4\pi L_V} \tag{2}$$

where L_H and L_V are horizontal and vertical image lengths and wavelength $\lambda = 0.633$ µm. The pixel length on the surface of the step gauge corresponds to 47.12 µm which was measured by comparing the number of pixels with a known length where 191 pixels correspond to 9000 µm.

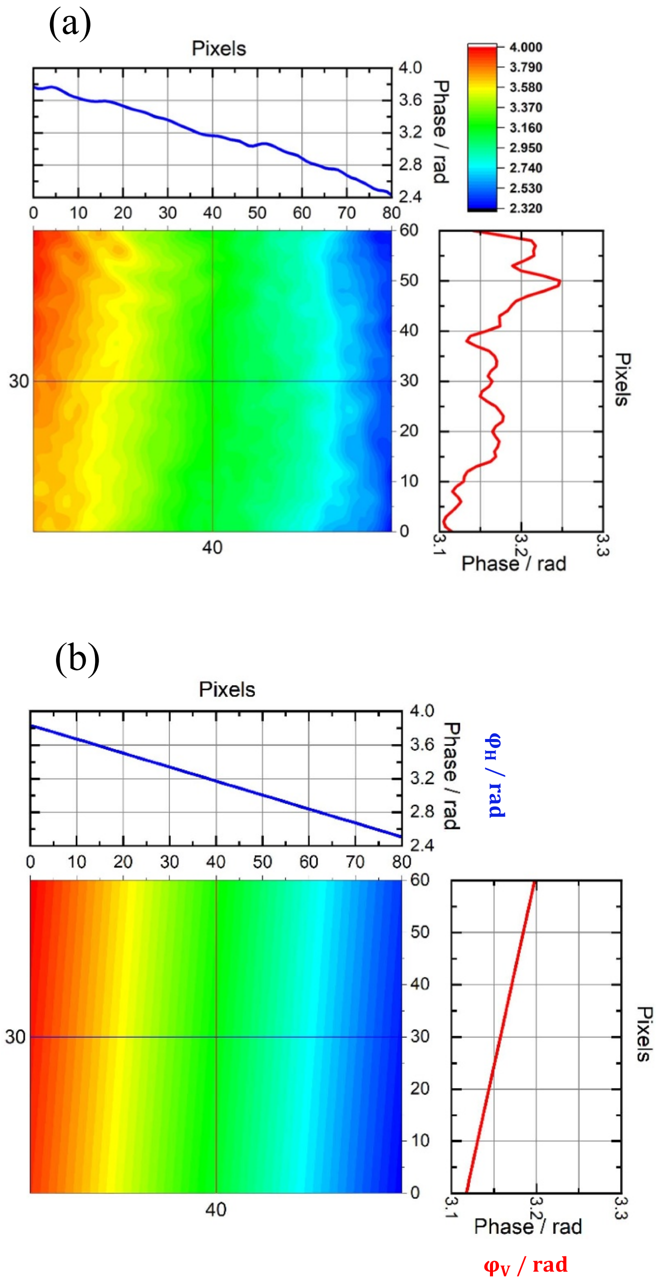

Figure 4. An example of phase information retrieval for nearly normal beam incidence condition through (a) unwrapped phase map of SG_R. (b) The resultant plane fitted phase map of SG_R. The blue and red lines in the horizontal and vertical profile graphs provide information on the interferometric phase changes $\Delta\varphi_H$ and $\Delta\varphi_V$, to estimate the tilt angles due to yaw and pitch, respectively.

3. Theoretical model description

We summarize our theoretical approach to interpret the working principle of the purpose-made optical system consisting of the mirror array and the alignment monitoring mirror suitable for measuring parallelism between two reflective surfaces forming a rectangular slot-like structure. A detailed description of the theoretical study is presented in the appendix. The analysis is based on a ray tracing model which explains the alignment sensitivity of the optical system. The rotations of the optical system and the step gauge, about X and Y axes, alter the detected tilt. The tilt of the step gauge and of the mirror array with the attached alignment mirror, are the main sources of misalignments during the measurement. The optical system needs to be translated along Y axis to enter each step gauge opening and along Z axis to access the next step gauge opening after finishing measurement in the previous position. Hence, the misalignments due to the movements of the mirror array can be tracked from M5. The reference surface can suffer pitch and yaw misalignment which can be monitored from the phase image of SG_R. For the following analysis, we assume that the mirror array is inside the first step gauge opening with M7 and M6 facing SG_{E2} and SG_{O3}, respectively. To methodically observe the effects in the corresponding sensitivities of the optical system under both aligned and misaligned conditions of the mirror array and the step gauge, the entire analysis is carried out by considering the primary incident ray direction along Z axis.

For the attached alignment mirror M5 of the optical system, the angles θ''_{M_5} and ψ''_{M_5} formed between the incident and the reflected ray due to pitch (θ) and yaw (ψ) are 2θ and 2ψ, respectively, (explained in appendix A.1). If the optical system is rotated by a small angle θ due to pitch, the direction of the reflected ray from M6 or M7 via M4 is the same as in the condition of the mirror array when no misalignment is present (appendix A.2). It is in accordance with the expected result as mirrors M4 and M7 are positioned as a triangular prism reflector-like arrangement and mirrors M4 and M6 are forming a periscope. If the optical system is rotated by a small angle ψ to introduce yaw misalignment, the direction of the reflected ray from M6 via M4 is again similar to the condition when the tilt is not introduced which is the expected property of reflections of mirrors M4 and M6. However, the angle ($\psi''_{SG_{E2}}$) between the incident and the reflected ray for the surface SG_{E2} facing M7 due to yaw misalignment of the optical system is 4ψ (detailed in appendix A.2). Hence, the theoretical analysis suggests that the surface tilt measurement process for SG_{E2} and SG_{O3} with M7 and M6 is not sensitive to the tilt of the optical system due to pitch. For yaw, only M7 shows sensitivity to the system tilt while measuring SG_{E2}, however, M6 does not show any ray deviation due to yaw misalignment. The theoretical analysis provides the sensitivity due to yaw for M7, i.e.,

$$\psi''_{SG_{E2}}/\psi''_{M_5} = 2 \tag{3}$$

when compared with M5. The tilt correction factor of the optical system is required to enable parallelism measurement of step gauge faces with improved accuracy.

Apart from the optical system, changes in the interference fringe pattern can be observed due to the misalignment of the step gauge. If the step gauge suffers yaw and pitch misalignment, the consequent changes in the interference fringe patterns can be detected from SG_R, SG_{E2} and SG_{O3}. The sensitivity analysis due to the step gauge alignment is presented in appendix (appendix B).

4. Experimental result

The experimental results presented in this section are obtained for alignment sensitivity estimation due to the misalignment of (a) the optical system with mirror array and the alignment mirror and (b) step gauge. The interferogram analysis was performed by phase stepping method as described in section 2.2. The experimental data of pitch and yaw sensitivities for both the optical system and step gauge are compared with the theoretical prediction (section 3). The performance of the optical system for measuring the surface parallelism of seven surfaces of a step gauge is presented in section 4.3.

4.1. Alignment sensitivity due to optical system and comparison with theoretical analysis

A step gauge was placed in the measurement arm of the interferometer. The reference front surface SG_R, as shown in figure 1, was first aligned normal to the incident beam. After that, the aligned optical system with the mirror array was moved by downward translation to enter the first step gauge opening with the two surfaces SG_{E2} and SG_{O3}. The system was adjusted for normal beam incidence by observing the fringe pattern of surface of M5 (figure 2).

Next, the alignment sensitivity due to the optical system was checked by introducing pitch and yaw. The changes in the fringe pattern introduced by the system were studied utilizing the phase stepping method. Figure 5 depicts the experimental outcome on how the tilt angles of SG_{E2} and SG_{O3} monitored via M7 and M6 depend on the surface tilt angle of M5 due to pitch and yaw misalignment of the optical system. Primed angle symbols indicate that they are obtained from the interferometric images and do not necessarily correspond to a change of the actual physical state of the step gauge. After introducing yaw, vertical fringes appeared due to the response of surface M_5 via M5 and surface SG_{E2} via mirrors M4 and M7. To check the response, the amount of yaw was increased and corresponding changes in the phase images were measured for all surfaces. The result suggests that only SG_{E2} and M5 respond to yaw misalignment of the optical system but SG_{O3} does not show any response. This is in accordance with the theoretical analysis. Similarly, after adjusting the setup for normal beam incidence, the pitch misalignment was gradually introduced. For pitch, both M7 and M6 did not show any response as there were no changes in the phase images observed for SG_{E2} and SG_{O3}. However, response from Mirror M5 was present.

According to the theoretical prediction, along with surface M_5, only SG_{E2} via M7 but not SG_{O3} via M6 will respond to the yaw misalignment of the optical system. For pitch misalignment of the system, both SG_{E2} and SG_{O3} are unresponsive. The experimental outcome in figure 5 confirms the prediction. The linear dependence of the angle $\psi'_{SG_{E2}}$ on the corresponding tilt angle ψ_{M_5} due to M_5 is present in the experimental results for yaw misalignment. With a linear fit through the experimental data points, the sensitivity for yaw can be estimated. The experimental data suggest $\psi'_{SG_{E2}}/\psi_{M_5} \sim 2$, implying $\psi''_{SG_{E2}}/\psi''_{M_5} \sim 2$ which agrees with the theoretical prediction as presented in equation (3). The estimated correction factor is required for the calculation of surface parallelism of the step gauge in order to eliminate the effect of the misalignment of the optical system.

4.2. Alignment sensitivity due to step gauge and comparison with the expected results

The measurements are also sensitive to the misalignments of the step gauge. Hence, we carried out measurements to check the corresponding alignment response by observing the changes in the phase images from SG_R, SG_{E2} and SG_{O3}. The phase image of M_5 under this condition remained unchanged. Figure 6 shows the experimental sensitivities due to step gauge tilt. Both pitch and yaw misalignment of the step gauge produced linear changes in the phase images for SG_R, SG_{E2} and SG_{O3}. Dashed lines indicate the expected relation between the angles of the step gauge surfaces considering a possible initial offset.

For the purpose of the uncertainty analysis, we estimate the scatter of the data around the expected results. The standard deviation between the dashed lines and corresponding measured data in figures 5 and 6 is 8 µrad. This standard deviation represents the uncertainty due to plane fitting of non-ideal step gauge surfaces.

4.3. Step gauge surface parallelism measurement

For surface parallelism measurement the step gauge was adjusted to align SG_R for normal beam incidence. The optical system was placed inside three successive step gauge openings to measure the parallelism of seven surfaces including the reference surface. At each position of the system, phase stepping data acquisition was performed. The phase images were analyzed, and surface tilts were calculated.

Considering the offset of the mirror array (section 2.1, figure 3(c)) and the corrections due to the alignment sensitivities, the angle of the surface tilt relative to the reference surface is calculated using equations (4)–(7),

$$\psi_{SG_{Ei}} = \psi'_{SG_{Ei}} - \psi_{SG_R} + 2\psi_{M_5} - \psi_{offset_{Ei}} \tag{4}$$

$$\theta_{SG_{Ei}} = \theta'_{SG_{Ei}} - \theta_{SG_R} - \theta_{offset_{Ei}} \tag{5}$$

$$\psi_{SG_{Oi}} = \psi'_{SG_{Oi}} - \psi_{SG_R} - \psi_{offset_{Oi}} \tag{6}$$

$$\theta_{SG_{Oi}} = \theta'_{SG_{Oi}} - \theta_{SG_R} - \theta_{offset_{Oi}}. \tag{7}$$

Parameters ψ_S and θ_S represent corrected yaw and pitch angle of surface S, where S can be M_5, SG_R, SG_{Ei}, SG_{Oi}, $offset_{Ei}$ and $offset_{Oi}$. Angles ψ'_S and θ'_S are the measured surface tilt angles, before applying the corrections. The surface tilt of SG_R is required for reference surface tilt removal. The offset values for the measurement of the even step gauge surfaces with face number $i = 2, 4, 6\ldots$, are $\psi_{offset_{Ei}} = 3$ µrad and $\theta_{offset_{Ei}} = 15$ µrad. The corresponding offset values for measuring odd numbered step gauge faces with $i = 3, 5, 7\ldots$,

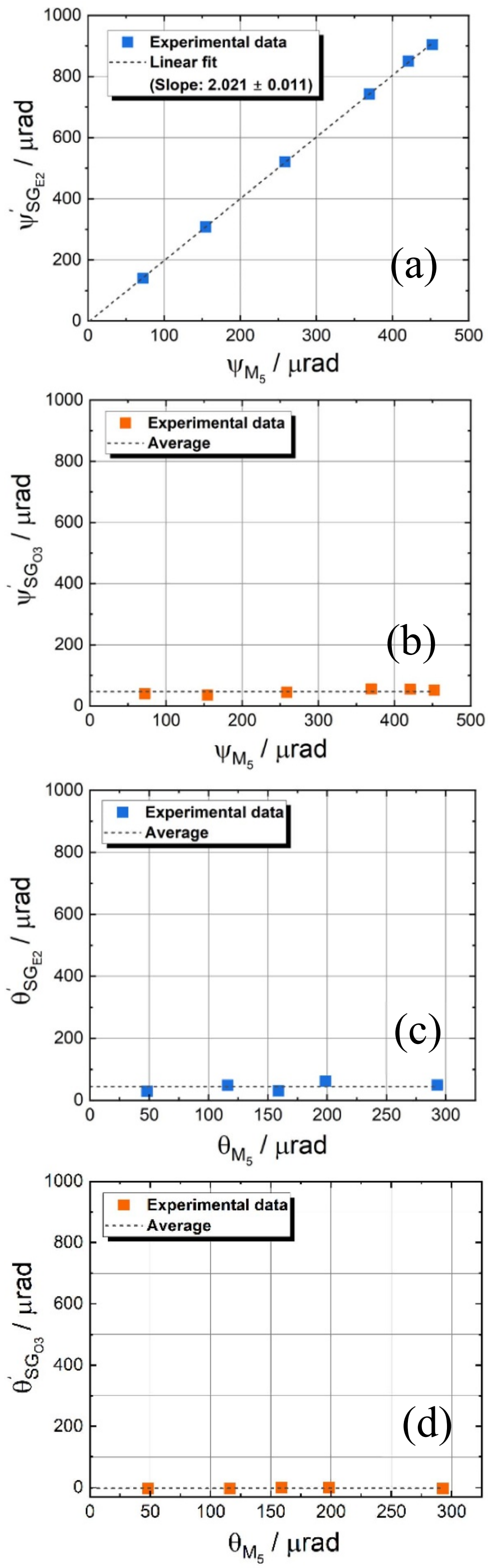

Figure 5. Experimental results on the sensitivities due to (a), (b) yaw and (c), (d) pitch misalignment of the optical system with mirrors M4, M7 (facing SG_{E2}) and M6 (facing SG_{O3}) of the mirror array. Parameters $\psi'_{SG_{E2}}$, $\psi'_{SG_{O3}}$, $\theta'_{SG_{E2}}$ and $\theta'_{SG_{O3}}$ denote the apparent tilt angles for SG_{E2} and SG_{O3} due to yaw and pitch misalignment of the mirror array and ψ_{M_5} and θ_{M_5} are the corresponding tilt angles of alignment mirror M5. Both M6 and M7 are not sensitive to pitch misalignment of the mirror array. The slope of the linear fit in (a) indicates the correction factor required to measure the tilt angles of step gauge faces SG_{Ei}, due to yaw misalignment of the mirror array. Angles $\psi'_{SG_{O3}}$, $\theta'_{SG_{E2}}$ and $\theta'_{SG_{O3}}$ are non-zero due to experimental offsets in (b)–(d). The standard uncertainty is smaller than the size of the data points.

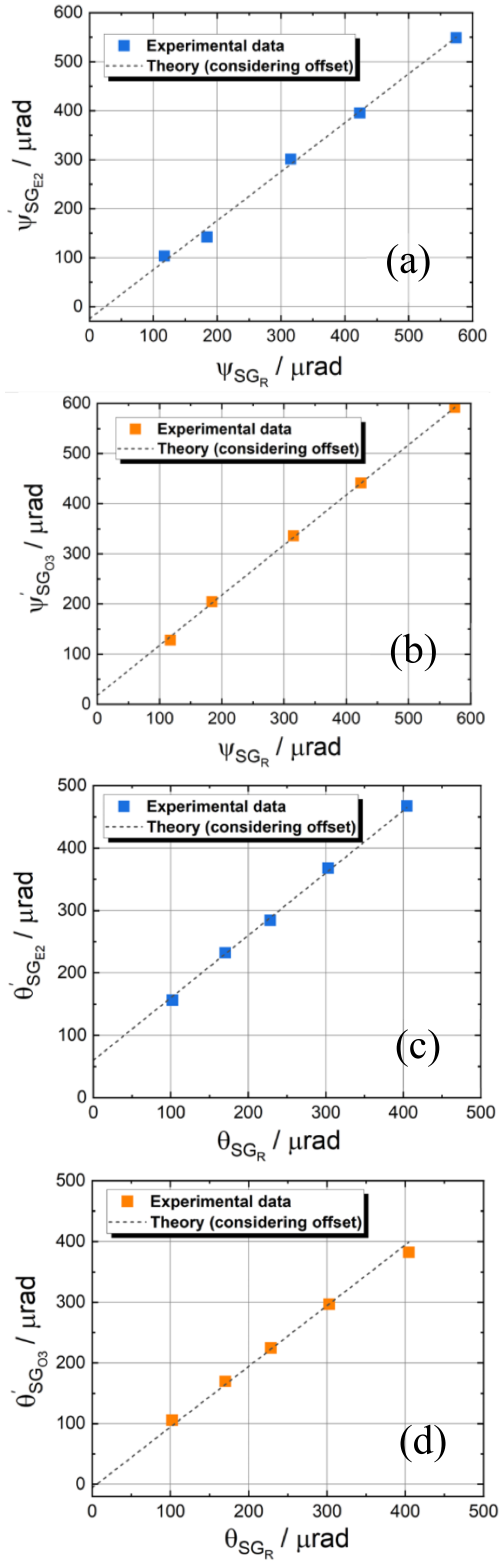

Figure 6. Experimental results on the sensitivities due to (a), (b) yaw and (c), (d) pitch misalignment of the step gauge. Parameters $\psi'_{\mathrm{SG_{E2}}}$, $\psi'_{\mathrm{SG_{O3}}}$, $\theta'_{\mathrm{SG_{E2}}}$ and $\theta'_{\mathrm{SG_{O3}}}$ denote the tilt angles of SGE2 and SGO3 and $\psi_{\mathrm{SG_R}}$, $\theta_{\mathrm{SG_R}}$ are the tilt angles of $\mathrm{SG_R}$ due to yaw and pitch misalignments of the step gauge, respectively. The dashed line on each graph represents the theoretical behavior. The offset was calculated from the graphs and considered for presenting the dashed lines. Size of the data points corresponds to the standard uncertainty.

are $\psi_{\mathrm{offset_{O\mathit{i}}}} = 27$ µrad and $\theta_{\mathrm{offset_{O\mathit{i}}}} = 2$ µrad. In figures 5(c) and 6(c), the average intercept is about 50 µrad, which is larger than the offset $\theta_{\mathrm{offset_{E\mathit{i}}}} = 15$ µrad, while in other cases the intercepts and offsets approximately agree. Offset $\theta_{\mathrm{offset_{E\mathit{i}}}}$ appears to have increased by 35 µrad between the initial offset measurement and the measurements of figures 5 and 6.

Table 1. Measurement of step gauge (SG) surface parallelism.

SG surface (S)	ψ_{M_5}/µrad	Measured tilt angle of SG surface/µrad ψ'_S	θ'_S	Corrected value of SG surface tilt angle/µrad ψ_S	θ_S
SG_R		28	1	0	0
SG_{E2}	8	12	12	−3	−4
SG_{O3}		17	−11	−38	−14
SG_R		30	−1	0	0
SG_{E4}	5	18	70	−5	56
SG_{O5}		31	29	−26	28
SG_R		33	−1	0	0
SG_{E6}	28	−18	66	2	52
SG_{o7}		23	1	−37	0

Table 1 shows the obtained results of parallelism measurement carried out between the initial offset measurement and the measurements of figures 5 and 6. The + sign of the angle denotes anticlockwise rotation and the − sign is for clockwise rotation of the step gauge surfaces. The step gauge reference surface SG_R changes only very little while measuring with the optical system at the three different SG openings. The highest angular deviation was 56 µrad for $\theta_{SG_{E4}}$. The estimated axial distance change is 0.14 µm, at quarter of the height from the top edge of SG_{E4} (i.e., 2.5 mm) with the above-mentioned pitch angle change of 56 µrad. The measurement to test the parallelism of the step gauge faces was repeated 2 weeks after the measurements of table 1 and figures 5, 6. The resulting value of standard deviation between the first measurement (table 1) and the repeat measurement was 44 µrad for θ_S of even surfaces SG_{E2}, SG_{E4} and SG_{E6}, which corresponds to the observed change of 35 µrad in $\theta_{\mathrm{offset}_{Ei}}$ between the initial offset measurement and the measurements of figures 5 and 6. For other surfaces and angles the standard deviation due to repeatability was 12 µrad.

The standard uncertainty due to the plane fitting analysis in the primed angle quantities of equations (4)–(7) was estimated in section 4.2 as 8 µrad. A similar independent uncertainty component is assigned to angles ψ_{SG_R} and θ_{SG_R}. Remaining terms in equations (4)–(7) are determined by reflections from mirror surfaces. The effect of non-ideal alignment of mirror assembly M4, M6 and M7 is taken into account by angular offset corrections determined using the method described in section 2. These angular corrections are conservatively assumed to have the same uncertainties as in the plane fitting of non-ideal step gauge surfaces, although mirror surfaces, in general, are of better planarity than step gauge surfaces. Combining quadratically the three uncertainty components, gives 14 µrad as the uncertainty of the left-hand side of equations (4)–(7). Considering the above-mentioned standard deviation of 12 µrad due to the repeatability and the standard uncertainty of 14 µrad yields the combined standard uncertainty of 18 µrad for the parallelism measurement of the step gauge surfaces in table 1.

5. Conclusion

An interferometric approach for measuring the surface parallelism of step gauges has been presented in this study. With an optical system consisting of a mirror array which is a combination of a periscope and a triangular prism reflector-like arrangement, the phase images of the step gauge faces were recorded and corresponding angle deviations of the faces from the reference front surface were estimated. Alignment sensitivity of the system is an important aspect of the entire measurement process to compensate misalignment induced errors. The alignment sensitivity was checked by introducing pitch and yaw misalignment to the optical system and the step gauge. The experimentally obtained results of the system agree well with the theoretical analysis. From the sensitivities, the correction factors of the measurements were calculated, which are necessary to obtain the correct parallelism information of the step gauge surfaces. The presented demonstration interferometric setup for measuring the surface parallelism of step gauges allows the identification and monitoring of the misalignment related measurement errors even though the adjustments to position the mirror array were carried out with manual control. This feasibility study shows the potential of the presented method to work as a suitable solution for performing non-contact parallelism measurements of step gauge faces.

Acknowledgments

This work was supported by Academy of Finland Flagship Programme, Photonics Research and Innovation (PREIN), Finland, (Decision No. 320167).

Appendix

A. Alignment sensitivity due to the optical system

A.1. Alignment mirror M5 sensitivity

Directions of the reflections from M5 mirror and step gauge surfaces are derived in this Appendix. The co-ordinate system

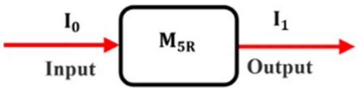

Figure A1. Block diagram of measurement beam interaction with the alignment monitoring mirror M5 under the condition when misalignment is not introduced to the optical system.

indicated in figures 1 and 2 is used. The mirror surface normal M and the incident and reflected ray vectors are denoted by I_0 and I_1, respectively. Following the law of reflection,

$$I_1 = M_R I_0, \tag{A1}$$

$$M_R = I - 2\,M\,M^T = \begin{bmatrix} 1-2M_x{}^2 & -2M_xM_y & -2M_xM_z \\ -2M_yM_x & 1-2M_y{}^2 & -2M_yM_z \\ -2M_zM_x & -2M_zM_y & 1-2M_z{}^2 \end{bmatrix} \tag{A2}$$

where M_R is the mirror matrix, I is the identity matrix, $M = \begin{bmatrix} M_x \\ M_y \\ M_z \end{bmatrix}$ and superscript T denotes transpose. As schematically presented in figure A1 for alignment monitoring mirror M5 of the optical system, the surface normal M_5 is pointing along $-Z$ axis, $M_{5x} = 0, M_{5y} = 0, M_{5z} = -1$, and the incident ray is directed along $+Z$ axis,
hence,

$$M_{5R} = \begin{bmatrix} 1 & 0 & 0 \\ 0 & 1 & 0 \\ 0 & 0 & -1 \end{bmatrix} \tag{A3}$$

and applying (A1),

$$I_1 = M_{5R} I_0$$

or

$$\begin{bmatrix} I_{1x} \\ I_{1y} \\ I_{1z} \end{bmatrix} = \begin{bmatrix} 0 \\ 0 \\ -1 \end{bmatrix}. \tag{A4}$$

If the mirror is rotated by a small angle θ about X axis to introduce pitch misalignment, then with new mirror matrix after the rotation, the output is

$$I_1 = R_\theta M_{5R} R_\theta{}^T I_0, \tag{A5}$$

where R_θ is the rotation matrix along X axis,

$$R_\theta = \begin{bmatrix} 1 & 0 & 0 \\ 0 & \cos(\theta) & -\sin(\theta) \\ 0 & \sin(\theta) & \cos(\theta) \end{bmatrix}. \tag{A6}$$

According to equation (A5),

$$\begin{bmatrix} I_{1x} \\ I_{1y} \\ I_{1z} \end{bmatrix} = \begin{bmatrix} 0 \\ \sin(2\theta) \\ -\cos(2\theta) \end{bmatrix}. \tag{A7}$$

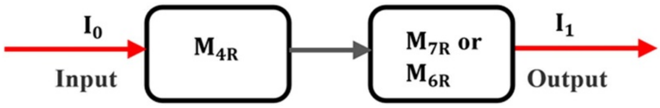

Figure A2. Block diagram of measurement beam interaction with the mirror array: M4, M7 and M6, under the condition when misalignment is not introduced to the optical system.

If the mirror is rotated by a small angle ψ about Y axis, then due to yaw, the rotation matrix is

$$R_\psi = \begin{bmatrix} \cos(\psi) & 0 & \sin(\psi) \\ 0 & 1 & 0 \\ -\sin(\psi) & 0 & \cos(\psi) \end{bmatrix} \tag{A8}$$

and

$$\begin{bmatrix} I_{1x} \\ I_{1y} \\ I_{1z} \end{bmatrix} = \begin{bmatrix} -\sin(2\psi) \\ 0 \\ -\cos(2\psi) \end{bmatrix}. \tag{A9}$$

The angles between the incident and the reflected ray for pitch (θ) or yaw (ψ) misalignments of M5 are 2θ and 2ψ, respectively.

A.2. Sensitivity of the mirror array

The mirror normal of M4 makes 45° angle with Z axis and directs the incident ray towards the reflective surfaces M6 and M7 to produce the output I_1, as represented in the block diagram of figure A2. Hence,

$$M_{4R} = \begin{bmatrix} 1 & 0 & 0 \\ 0 & 0 & -1 \\ 0 & -1 & 0 \end{bmatrix}. \tag{A10}$$

For mirror M6, which is facing SG_{O3},

$$M_{6R} = \begin{bmatrix} 1 & 0 & 0 \\ 0 & 0 & -1 \\ 0 & -1 & 0 \end{bmatrix}. \tag{A11}$$

For incident ray I_0 which is directed along $+Z$ axis, the output

$$I_1 = M_{6R}\, M_{4R}\, I_0 \tag{A12}$$

or

$$\begin{bmatrix} I_{1x} \\ I_{1y} \\ I_{1z} \end{bmatrix} = \begin{bmatrix} 0 \\ 0 \\ 1 \end{bmatrix}. \tag{A13}$$

Similarly, for mirror M7, which is facing SG_{E2},

$$M_{7R} = \begin{bmatrix} 1 & 0 & 0 \\ 0 & 0 & 1 \\ 0 & 1 & 0 \end{bmatrix}. \tag{A14}$$

For incident ray I_0, which is directed along $+Z$ axis, the output is,

$$I_1 = M_{7R} M_{4R} I_0 \tag{A15}$$

or

$$\begin{bmatrix} I_{1x} \\ I_{1y} \\ I_{1z} \end{bmatrix} = \begin{bmatrix} 0 \\ 0 \\ -1 \end{bmatrix}. \tag{A16}$$

If the optical system is rotated by a small angle θ due to pitch, then the output I_1 due to mirror assembly M4 and M6 is

$$I_1 = R_\theta M_{6R} R_\theta^{T} R_\theta M_{4R} R_\theta^{T} I_0 \tag{A17}$$

or

$$\begin{bmatrix} I_{1x} \\ I_{1y} \\ I_{1z} \end{bmatrix} = \begin{bmatrix} 0 \\ 0 \\ 1 \end{bmatrix}. \tag{A18}$$

The direction of the reflected ray (A18) is along $+Z$ axis corresponding to a similar situation when no pitch misalignment was introduced (according to A13).

For another reflective surface of the mirror array, M7 facing the SG_{E2}, the output due to pitch for the combined effect of M4 and M7 is

$$I_1 = R_\theta M_{7R} R_\theta^{T} R_\theta M_{4R} R_\theta^{T} I_0 \tag{A19}$$

or

$$\begin{bmatrix} I_{1x} \\ I_{1y} \\ I_{1z} \end{bmatrix} = \begin{bmatrix} 0 \\ 0 \\ -1 \end{bmatrix}. \tag{A20}$$

Hence, the direction of the reflected ray is along $-Z$ axis suggesting the same condition as in equation (A16), when tilt due to pitch was not introduced on the optical system. According to this analysis, if the system is misaligned due to pitch, then there will be no consequent fringe pattern changes due to SG_{E2} or SG_{O3}, however, M_5 will show response.

If optical system is rotated by a small angle ψ about Y axis for yaw misalignment and the incident ray is directed along $+Z$ axis, then the output due to M4 and M6 is

$$I_1 = R_\psi M_{6R} R_\psi^{T} R_\psi M_{4R} R_\psi^{T} I_0 \tag{A21}$$

or

$$\begin{bmatrix} I_{1x} \\ I_{1y} \\ I_{1z} \end{bmatrix} = \begin{bmatrix} 0 \\ 0 \\ 1 \end{bmatrix}. \tag{A22}$$

Hence, the reflected ray is following the same path as in the case of no yaw misalignment according to equation (A13).

For mirror M7 of the mirror array, the output I'_1 for the case of yaw (figure A3) is

$$I'_1 = R_\psi M_{7R} R_\psi^{T} R_\psi M_{4R} R_\psi^{T} I_0 \tag{A23}$$

Figure A3. Block diagram of measurement beam interaction with the mirrors M4 and M7 which faces SG_{E2} under the condition when the optical system is tilted due to yaw. The prime symbol ($'$) in this case represents mirror rotation about Y axis to introduce yaw.

or

$$\begin{bmatrix} I'_{1x} \\ I'_{1y} \\ I'_{1z} \end{bmatrix} = \begin{bmatrix} -\sin(2\psi) \\ 0 \\ -\cos(2\psi) \end{bmatrix}. \tag{A24}$$

The reflected ray from M7, and further reflected from SG_{E2}, is not following the same path as the incident ray. Surface SG_{E2} has surface normal along $+Z$ axis, which reflects the ray coming from M7. The mirror matrix of SG_{E2} and the corresponding output $I_{SG_{E2}}$ are

$$M_{SG_{E2}\_R} = \begin{bmatrix} 1 & 0 & 0 \\ 0 & 1 & 0 \\ 0 & 0 & -1 \end{bmatrix} \tag{A25}$$

and

$$I_{SG_{E2}} = M_{SG_{E2}\_R} I'_1 \tag{A26}$$

or

$$\begin{bmatrix} I_{SG_{E2}x} \\ I_{SG_{E2}y} \\ I_{SG_{E2}z} \end{bmatrix} = \begin{bmatrix} -\sin(2\psi) \\ 0 \\ \cos(2\psi) \end{bmatrix}. \tag{A27}$$

Finally, the back reflected ray from SG_{E2}, i.e., $I_{SG_{E2}}$ is the incident ray for the mirror assembly M7 and M4 to produce the output I_1 as shown in figure A3:

$$I_1 = R_\psi M_{4R} R_\psi^{T} R_\psi M_{7R} R_\psi^{T} I_{SG_{E2}} \tag{A28}$$

or

$$\begin{bmatrix} I_{1x} \\ I_{1y} \\ I_{1z} \end{bmatrix} = \begin{bmatrix} -\sin(4\psi) \\ 0 \\ -\cos(4\psi) \end{bmatrix}. \tag{A29}$$

The angle ($\psi''_{SG_{E2}}$) between the incident and the reflected ray at SG_{E2} due to yaw misalignment of the optical system, by angle ψ, is 4ψ.

B. Alignment sensitivity due to step gauge

Apart from the optical system, misalignment can occur due to the step gauge position. If the step gauge suffers yaw and pitch misalignment, then the consequent changes in the interference fringe pattern can be detected from the SG_R surface which is the reference surface during the measurement and also from SG_{E2} and SG_{O3} via M7 and M6, respectively. We assume that the mirror normal of M5 is aligned parallel with the incident

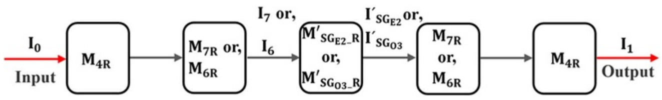

Figure A4. Block diagram of measurement beam interaction with the mirrors M4, M6 with surface SG_{O3} and M7 with surface SG_{E2}. The prime symbol ($'$) represents the condition when the step gauge is tilted i.e., step gauge rotation about X or Y axis to introduce pitch or yaw.

beam. Hence, in this analysis, the effect of step gauge misalignment on SG_{E2} and SG_{O3} is discussed (see figure A4). The response of SG_R is similar to that of M5 described in section A.1.

The normal of SG_{E2} points along $+Z$ direction ($M_{SG_{E2}x}=0$, $M_{SG_{E2}y}=0$, $M_{SG_{E2}z}=+1$) with mirror matrix $M_{SG_{E2}\_R}$ of equation (A25) and the incident ray along $-Z$ axis as in equation (A16) which is under the condition that misalignment of the optical system is not introduced. If yaw is introduced to the step gauge, then the new mirror matrix of surface SG_{E2} due to the rotation will produce output $I'_{SG_{E2}}$ from tilted SG_{E2},

$$I'_{SG_{E2}} = R_{\psi}\, M_{SG_{E2}\_R}\, R_{\psi}{}^{T}\, I_7 \tag{A30}$$

or

$$\begin{bmatrix} I'_{SG_{E2}x} \\ I'_{SG_{E2}y} \\ I'_{SG_{E2}z} \end{bmatrix} = \begin{bmatrix} \sin(2\psi) \\ 0 \\ \cos(2\psi) \end{bmatrix}. \tag{A31}$$

Ray $I'_{SG_{E2}}$ is the input of the mirrors M7 and M4 (which are not misaligned) to produce the output,

$$I_1 = M_{4R}\, M_{7R}\, I'_{SG_{E2}} \tag{A32}$$

or

$$\begin{bmatrix} I_{1x} \\ I_{1y} \\ I_{1z} \end{bmatrix} = \begin{bmatrix} \sin(2\psi) \\ 0 \\ -\cos(2\psi) \end{bmatrix}. \tag{A33}$$

If pitch is introduced to step gauge and the incident ray is coming along $-Z$ axis from M7 mirror of the mirror array which is under the condition that misalignment is not introduced, then with the mirror matrix $M'_{SG_{E2}\_R}$ and the corresponding output $I'_{SG_{E2}}$ due to pitch misalignment of surface SG_{E2}

$$I'_{SG_{E2}} = R_{\theta}\, M_{SG_{E2}\_R}\, R_{\theta}{}^{T}\, I_7 \tag{A34}$$

or

$$\begin{bmatrix} I'_{SG_{E2}x} \\ I'_{SG_{E2}y} \\ I'_{SG_{E2}z} \end{bmatrix} = \begin{bmatrix} 0 \\ -\sin(2\theta) \\ \cos(2\theta) \end{bmatrix}. \tag{A35}$$

Ray $I'_{SG_{E2}}$ is the input of the mirrors M7 and M4 (which are not misaligned) to produce the output,

$$I_1 = M_{4R}\, M_{7R}\, I'_{SG_{E2}} \tag{A36}$$

or

$$\begin{bmatrix} I_{1x} \\ I_{1y} \\ I_{1z} \end{bmatrix} = \begin{bmatrix} 0 \\ \sin(2\theta) \\ -\cos(2\theta) \end{bmatrix}. \tag{A37}$$

When the step gauge is not misaligned, the SG_{O3} surface normal points to $-Z$ direction ($M_{SG_{O3}x}=0, M_{SG_{O3}y}=0, M_{SG_{O3}z}=-1$) and the mirror matrix of SG_{O3} is

$$M_{SG_{O3}\_R} = \begin{bmatrix} 1 & 0 & 0 \\ 0 & 1 & 0 \\ 0 & 0 & -1 \end{bmatrix}. \tag{A38}$$

If the yaw is introduced to the step gauge, then the mirror matrix of SG_{O3} will produce output $I'_{SG_{O3}}$ from tilted SG_{O3}. The incident ray is along $+Z$ axis from mirror M6 and the corresponding output ray is

$$I'_{SG_{O3}} = R_{\psi}\, M_{SG_{O3}\_R}\, R_{\psi}{}^{T}\, I_6 \tag{A39}$$

or

$$\begin{bmatrix} I'_{SG_{O3}x} \\ I'_{SG_{O3}y} \\ I'_{SG_{O3}z} \end{bmatrix} = \begin{bmatrix} -\sin(2\psi) \\ 0 \\ -\cos(2\psi) \end{bmatrix}. \tag{A40}$$

Ray $I'_{SG_{O3}}$ is the input of the mirror assembly M6 and M4 (which are not misaligned) to produce the output

$$I_1 = M_{4R}\, M_{6R}\, I'_{SG_{O3}} \tag{A41}$$

or

$$\begin{bmatrix} I_{1x} \\ I_{1y} \\ I_{1z} \end{bmatrix} = \begin{bmatrix} -\sin(2\psi) \\ 0 \\ -\cos(2\psi) \end{bmatrix}. \tag{A42}$$

If pitch is introduced to the step gauge and the incident ray is coming from mirror M6, then the corresponding output $I'_{SG_{O3}}$ due to pitch misalignment of SG_{O3} is

$$I'_{SG_{O3}} = R_{\theta}\, M_{SG_{O3}\_R}\, R_{\theta}{}^{T}\, I_6 \tag{A43}$$

or

$$\begin{bmatrix} I'_{SG_{O3}x} \\ I'_{SG_{O3}y} \\ I'_{SG_{O3}z} \end{bmatrix} = \begin{bmatrix} 0 \\ \sin(2\theta) \\ -\cos(2\theta) \end{bmatrix}. \tag{A44}$$

Ray $I'_{SG_{O3}}$ is now the input of the mirror assembly M6 and M4 (which are not misaligned) to produce the output

$$I_1 = M_{4R}\, M_{6R}\, I'_{SG_{O3}} \tag{A45}$$

or

$$\begin{bmatrix} I_{1x} \\ I_{1y} \\ I_{1z} \end{bmatrix} = \begin{bmatrix} 0 \\ \sin(2\theta) \\ -\cos(2\theta) \end{bmatrix}. \tag{A46}$$

The angles $\theta''_{SG_{E2}}, \theta''_{SG_{O3}}, \psi''_{SG_{E2}}$ and $\psi''_{SG_{O3}}$, which are formed between the incident and the reflected rays from the surfaces SG_{E2} and SG_{O3} under pitch (θ) and yaw (ψ) misalignment of the step gauge, are 2θ and 2ψ, respectively.

ORCID iDs

Sucheta Sharma https://orcid.org/0000-0002-4617-6146
Antti Lassila https://orcid.org/0000-0002-6991-7082

References

[1] Ikonen E, Kauppinen J, Korkolainen T, Luukkainen J and Riski K 1991 Interferometric calibration of gauge blocks by using one stabilized laser and a white-light source *Appl. Opt.* **30** 4477–8
[2] Boensch G 2001 Automatic gauge block measurement by phase stepping interferometry with three laser wavelengths *Proc. SPIE* **4401** 1–10
[3] Ikonen E and Riski K 1993 Gauge-block interferometer based on one stabilized laser and a white-light source *Metrologia* **30** 95–104
[4] Coveney T 2020 A review of state-of-the-art 1D length scale calibration instruments *Meas. Sci. Technol.* **31** 042002
[5] Petrò S and Moroni G 2021 A statistical point of view on the ISO 10360 series of standards for coordinate measuring systems verification *Measurement* **172** 108937
[6] Schödel R, Yacoot A and Lewis A 2021 The new *mise en pratique* for the metre—a review of approaches for the practical realization of traceable length metrology from 10^{-11} m to 10^{13} m *Metrologia* **58** 052002
[7] Castro H F F and Burdekin M 2003 Dynamic calibration of the positioning accuracy of machine tools and coordinate measuring machines using a laser interferometer *Int. J. Mach. Tools Manuf.* **43** 947–54
[8] Weichert C, Bütefisch S, Köning R and Flügge J 2017 Integration of a step gauge measurement capability at the PTB nanometer comparator concept and preliminary tests *MacroScale* (https://doi.org/10.7795/810.20180323G)
[9] Hsieh T-H, Huang H-L, Jywe W-Y and Liu C-H 2014 Development of a machine for automatically measuring static/dynamic running parallelism in linear guideways *Rev. Sci. Instrum.* **85** 035115
[10] Coveney T *et al* 2020 Calibration of 1-D CMM artefacts: step gauges (EURAMET.L-K5.2016) *Metrologia* **57** 04002
[11] Byman V, Jaakkola T, Palosuo I and Lassila A 2018 High accuracy step gauge interferometer *Meas. Sci. Technol.* **29** 054003
[12] Šafarič J, Klobučar R and Ačko B 2021 Measurement setup and procedure for precise step gauge calibration *IEEE Trans. Instrum. Meas.* **70** 1–10
[13] Yujiu S, Shiqing X, Feng Q, Yongqian L and Zili Z 2021 A non-contact calibration system for step gauges using automatic collimation techniques *Meas. Sci. Technol.* **32** 035011
[14] Kruger O A 2001 High-accuracy interferometric measurements of flatness and parallelism of a step gauge *Metrologia* **38** 237–40
[15] Kruger O A 2001 Investigation into the measuring of the length spacing of step gauges *Proc. SPIE* **4401** 70–82
[16] Servin M, Estrada J C and Quiroga J A 2009 The general theory of phase shifting algorithms *Opt. Express* **17** 21867–81
[17] Byman V and Lassila A 2015 MIKES' primary phase stepping gauge block interferometer *Meas. Sci. Technol.* **26** 084009